Group Differences in Time-Frequency Relevant Patterns for User-Independent BCI Applications

L. F. Velasquez-Martinez[1(✉)], F. Y. Zapata-Castaño[1], J. I. Padilla-Buritica[1,2], José Manuel Ferrández Vicente[2], and G. Castellanos-Dominguez[1]

[1] Signal Processing and Recognition Group, Universidad Nacional de Colombia, Manizales, Colombia
lfvelasquezm@unal.edu.co

[2] Universidad Politécnica de Cartagena, Cartagena, Spain

Abstract. We present a comparison of two known methodologies for group analysis in EEG signals, which are the analysis by Group ICA on synchronization and desynchronization ERS/ERD, and brain connectivity analysis by measuring wPLI, both analyzes based on the brain synchronization information. For comparison, we have taken into account different frequency bands related to sensorimotor stimuli and time segmentation in order to overcome the nonstationarity of the EEG signal. In addition, we have used a threshold algorithm to reduce the dimension of the connectivity matrix, conserving the connections that are most important for both methodologies. The results obtained from the BCI competition IV-2a database show that the variable can be measured between two different measurement spaces, using the Euclidean distance, conserving spatial zones with more meaningful physiological interpretation.

Keywords: Event-related Synchronization/Desynchronization · Functional connectivity · Group analysis · wPLI

1 Introduction

The brain is a vastly complex network of interconnected elements, having different brain regions interacting in the resting state as well as in response to a given stimulus or task by synchronization of oscillatory activities. In this regard, brain response could be useful in the development of Media and Information literacy applications. Functional connectivity is defined as the temporal correlation of neural activity between brain regions, measured by functional MRI, magneto or electroencephalography (MEG/EEG) signals that are very convenient because of their low cost and high temporal resolution.

Among the widely used applications, computer-based technologies are employed to communicate the brain with external devices. In particular, Motor Imagery (MI) is a mental process by which an individual rehearses or simulates

J. M. Ferrández Vicente et al. (Eds.): IWINAC 2019, LNCS 11486, pp. 138–145, 2019.
https://doi.org/10.1007/978-3-030-19591-5_15

some actions without involving muscle activities [2]. This cognitive neuroscience paradigm operates the signals measured from the sensorimotor cortex regions, which are the most directly linked to the motor output pathway in the brain, assuming that the imagination of movement execution attenuates the brain sensorimotor rhythms (SMRs).

Here, with the aim of enhancing the interpretation of MI tasks, we develop a group-level comparison between two different methods to analyze the synchronization, ss a result, the use of thresholding allows performing a reduced set of relevant brain connections, but with enough confidence to construct a meaningful explanation in time and frequency of the brain activity [3,4].

Although further adaptations are to be performed to optimally address the sources of inter-subject and inter-trial variance commonly found in EEG recordings, the presented group-level approach can be considered valid and promising to infer the latent structure of multi-subject datasets [5].

2 Materials

2.1 EEG Database and Preprocessing

We carry out experimental validation using the Dataset 2a from the BCI Competition IV, publicly available at[1], holding EEG signals recorded from nine subjects and measured with a 22-channels montage. All signals are sampled at $F_s = 250$ Hz and bandpass-filtered between 0.5 and 100 Hz. The dataset holds a trial set of four MI tasks, i.e., left hand, right hand, both feet, and tongue. The recordings were carried out in six runs separated by short breaks. Each run contained $N = 48$ trials lasting of 7 s and distributed. A short beep indicated the trial beginning followed by a fixation cross that appeared on the black screen within the first 2 s. Further, as the cue, an arrow (pointing to the left, right, up or down) appeared during 1.25 s, indicating the each MI task to imagine: left hand, right hand, both feet or tongue movement, respectively. In the following time interval, ranging from 3.25 to 6 s, each subject performed the demanded MI task while the cross re-appeared. In our analysis, a bi-class task (left and right hand) set is used, from which artifacts had been removed previously.

As a result, we have a set of N raw EEG data trials $\mathcal{X} = \{\boldsymbol{X}_n : r = 1, \ldots, N \in \mathbb{N}\}$ together with the respective class label set $\mathcal{L} = \{l_n\}$, with $l_r \in \{l, l'\}$, where $\boldsymbol{X}_n \in \mathbb{R}^{C \times T}$ is n-th EEG trial, with $C \in \mathbb{N}$ channels and $T \in \mathbb{N}$ time samples. Over this raw data set, each raw EEG channel is band-pass filtered using 17 five-order overlapped bandpass Butterworth filters within the range 4 Hz to 40 Hz. Each filter bandwidth is adjusted to 4 Hz with overlapping rate at 2 Hz as suggested in [6].

2.2 Subject-Level Feature Extraction

At this stage, we compare the following two feature extraction methods:

[1] www.bbci.de/competition/iv/.

Event-Related Desynchronization/Synchronization. This change of the ongoing EEG is a somatotopical organized control mechanism that can be generated intentionally by mental imagery and is frequency band specific. Using each band-pass filtered event-related trial $\boldsymbol{X}_r^c$, the ERD/S estimation is performed by squaring of samples and averaging over EEG trials, computing the variational percentage (decrease or increase) in EEG signal power regarding a reference period, at specific frequency band f and sample t [7]:

$$\zeta_{ft} = (\xi_{ft} - \bar{\xi}_f)/\bar{\xi}_{f\,[\%]}, \quad t \in T \tag{1}$$

where $\xi_{ft} = \mathbb{E}\left\{|x_t^2|_{rf} \in \boldsymbol{x}_{rf} : \forall r\right\}$ is the power scatter averaged across the trial set and $\bar{\xi}_f = \mathbb{E}\left\{\xi_{ft} : \forall t \in \tau_R\right\}$ is the trial power scatter averaged on the reference interval τ_R.

Functional Connectivity Estimation. Weighted Phase Locking Index (wPLI) is commonly used for estimation of functional connectivity between two EEG channels, due to its nonparametric nature and easy implementation [1]. wPLI quantifies the asymmetry of phase difference distribution between two specific channels c, c' (with $\forall c, c' \in C, c \neq c'$), being defined within the recording time span $T \in \mathbb{R}^+$. Initially, the instantaneous phase difference $\Delta\Phi_{ft}(;c,c') \in \mathbb{R}[0,\pi]$ is the angle computed through the continuous wavelet transform coefficients $W_{ft}(;) \in \mathbb{R}^+$,

$$\Delta\Phi_{ft}(n;c,c') = \frac{W_{ft}(n;c)W_{ft}(n;c')}{|W_{ft}(n;c)||W_{ft}(n;c')|}, \, t \in T, \tag{2}$$

Thus, the pair-wise connectivity estimation $y_{ft}^s(c,c')$ for subject is computed as,

$$y_{f,\tau}^s(c,c'), = \frac{\left|\mathbb{E}\left\{|(\Delta\Phi_{f\tau}(n;c,c'))|\,\mathrm{sgn}\left(\Delta\Phi_{f\tau}(n;c,c')\right) : \forall n\right\}\right|}{\mathbb{E}\left\{|(\Delta\Phi_{f\tau}(n;c,c'))| : \forall n\right\}} \tag{3}$$

where notations sgn and $\mathbb{E}\{\cdot : \forall n\}$ stand for *sign* function and averaging operator over n, respectively. The metric is normalized to highlight the connectivity patterns generated by each induced stimulus, being each $y_{f\tau}^s(c,c')$ mean-value averaged over the trial set $\{n \in N\}$ and on a given baseline interval [8]. Accordingly, $\hat{y}_{f\tau}(c,c') = \mathbb{E}_s\left\{y_{f\tau}^s(c,c')\right\}$ contains the pair-wise connectivity measures of each subject group.

2.3 Group Independent Components Analysis

With the aim of inferring about the source configuration at the group-level, all components constantly expressed across subjects can be estimated using a single ICA decomposition, which is performed on aggregate data sets built from EEG recordings of multiple subjects. Specifically, provided the computed ERD/S of the k-th subject $\boldsymbol{Z}^k \in \mathbb{R}^{c \times T}$, the aggregate data set $\boldsymbol{Y} \in \mathbb{R}^{c \times (T * N_s)}$ is given by the temporal concatenation $\boldsymbol{Y} = [\boldsymbol{y}_1, ..., \boldsymbol{y}_k, ..., \boldsymbol{y}_{N_s}]$, with $k \in N_s$, being N_s the total number of subjects included in the analysis. Furthermore, we apply

centering and whitening via principal component analysis (PCA) to $\boldsymbol{Y}$, yielding the principal components $\boldsymbol{R}^\top \boldsymbol{Y}$, where $\boldsymbol{R}$ is the orthonormal transformation matrix obtained from PCA. Applying the basic ICA model to the preprocessed data leads to $\boldsymbol{R}^\top \boldsymbol{Y} = \boldsymbol{A}\boldsymbol{S}$ where $\boldsymbol{S} = [\boldsymbol{s}_1, \ldots, \boldsymbol{s}_k, \ldots, \boldsymbol{s}_{N_s}]$ is the matrix holding the temporally concatenated component time-courses of N_s subjects [3].

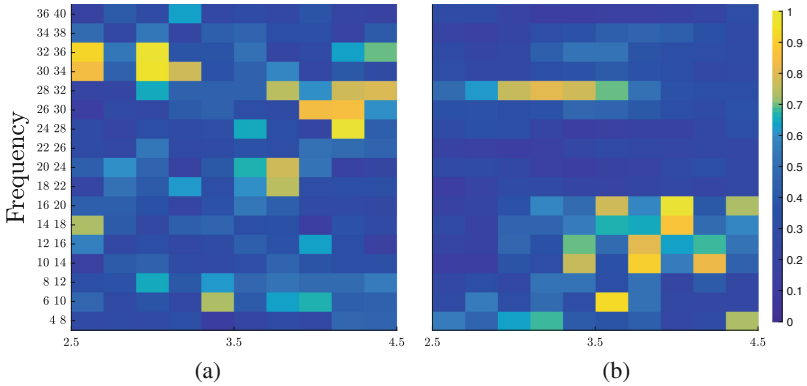

Fig. 1. Differences between classes from the estimated group patterns based on both methods Group-ICA (a) and connectivity (b).

3 Experimental Set-Up and Results

To measure the group differences in time-frequency relevant pattern, we perform a piecewise time segmentation. In each case of contrasting feature extraction, EEG and ERS/D, we split the whole time recording span (ranging from 2.5–4.5 s) into 10 segments, each one lasting 0.2 s. The segment length is adjusted, considering that a short segment leads to bias and variance at estimation level, while a long segment imposes a high computational load and restrain implementation on real-time system operation [9]. The subject analysis is carried out in the supervised mode, extracting separately the feature set for each class.

In the case of ERD/S, to estimate the variational percentage (decrease or increase) in EEG signal power regarding a reference period T_R, we fix $T_R = [0.5-1.5]$ s as in [10]. Accordingly, we build a matrix by class for each frequency band and time segment $\hat{\boldsymbol{Z}}_{f\tau} \in \mathbb{R}^{22\times 450}$ that holds the concatenated ERD/S response for all subjects. Afterward, ICA is applied by mean of the fastICA algorithm using a nonlinear tangent hyperbolic function to obtain $\hat{\boldsymbol{Y}}_{f\tau}^{g-ica} \in \mathbb{R}^{22\times 22}$ with columns holding the channel weights of the assessed independent components by class. In the case of functional connectivity extraction, we obtain a matrix $\hat{\boldsymbol{Y}}_{f,\tau}^{wpli} \in \mathbb{R}^{22\times 22}$ by mean of wPLI measure to encode the estimated pairwise changes in phase synchronization of the subject group.

As a result, the feature extraction stage provides a total of 170 matrices $\hat{\boldsymbol{Y}}_{f,\tau}$ by each class and estimated for all frequencies and time partitions. For the purpose of comparison, the contribution of across the channel set, at values τ and

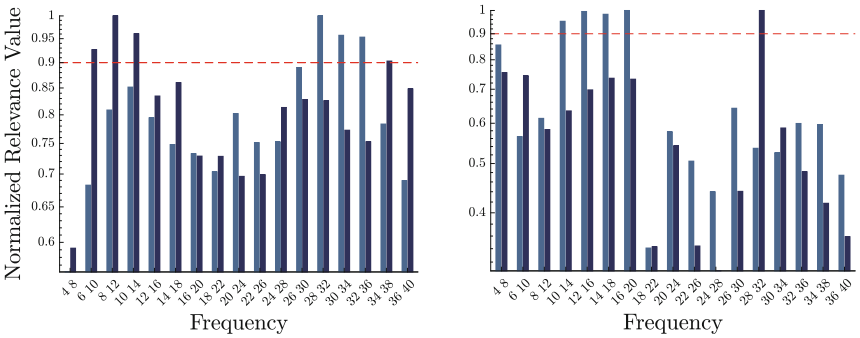

Fig. 2. Normalized frequency relevance value obtained based on both Group-ICA (left) and connectivity (right). – right class, – left class.

f, is assessed by $\boldsymbol{\rho}_{f,\tau} = \mathbb{E}_c\left\{\hat{\boldsymbol{Y}}_{f,\tau}\right\}$, being $\boldsymbol{\rho}_{f,\tau} \in \mathbb{R}^{22}$. However, the comparison is performed by averaging further the channel contribution across time, that is, $\eta_f = \mathbb{E}_\tau\left\{\|\boldsymbol{\rho}_{f,\tau}\|_2\right\}$, and yielding a vector contribution $\boldsymbol{\eta} \in \mathbb{R}^{17}$. $\|\cdot\|_2$ stands for ℓ_2-norm.

Further, using the conventional Euclidean distance, we assess the difference of contribution vectors between classes as seen in Fig. 1 that shows the normalized distances values. Besides, the marginal estimates of contribution by frequency are presented in Fig. 2, i.e., the normalized relevance values in terms of the frequencies that show more differences between time by class.

In this work, we consider as a relevant frequency the value overcoming 0.9. Accordingly, Figs. 3 and 4 exhibits the normalized time-frequency relevance values obtained for all channels by class for the selected relevant frequencies. Bright color designates high relevance values.

4 Discussion and Concluding Remarks

The estimation of cerebral synchronization and desynchronization allows highlighting the information contained in the domains of time and frequency. According to Fig. 1(a), we observe spurious differences for all segments and frequency bands with values lower than 0.7. However, the frequency bands from [24–28] Hz to [32–36] Hz shows high differences values in different time segments. Some lower differences are shown for the frequency bands [6–10] Hz and [14–18] Hz at different time segments. In the case of Fig. 1(b), we see a marked difference in the frequency [28–32] Hz the beginning of MI interval. However, we observe spurious differences for the end of MI period at frequencies belonging to μ band. However, we observe spurious differences for the end of MI period at frequencies belonging to μ band.

The contributions by frequency in Sect. 3, Group-ICA presents as the higher frequencies contributions in μ and β bands being the highest contributor the frequency band [8–12] Hz and [28–32] Hz, frequencies that are normally related

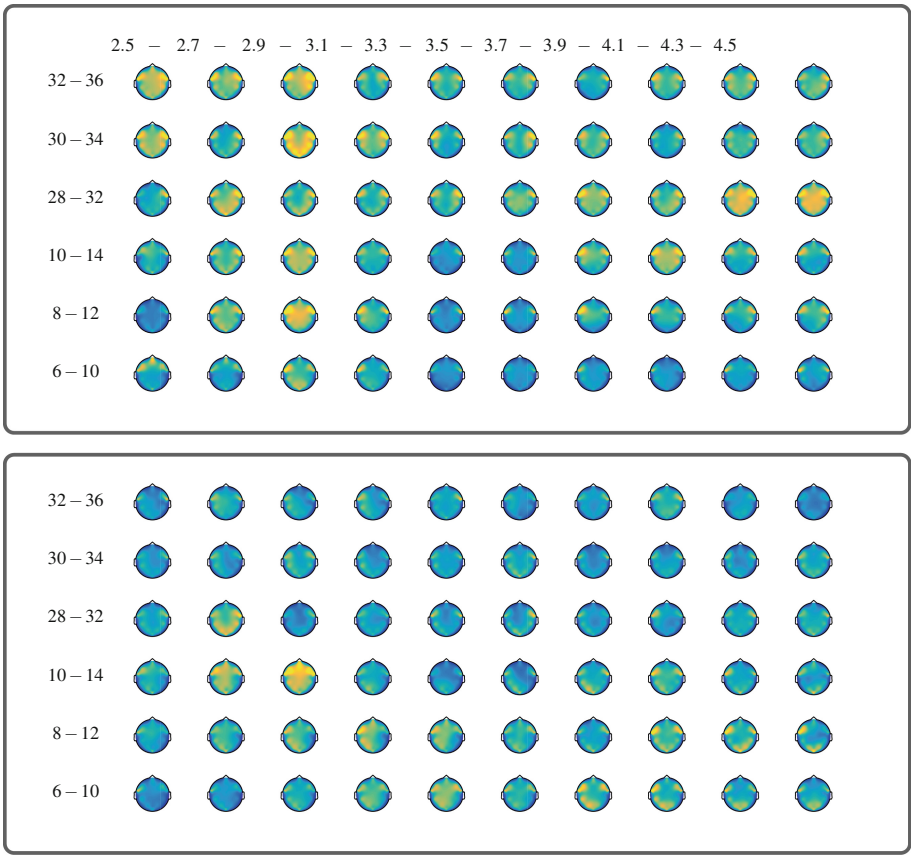

Fig. 3. Normalized time-frequency relevance values obtained by channel. Right class (first box) and left class (second box).

to MI tasks [10,11]. On the other hand, Sect. 3 shows the highest frequencies contributors in [16–20] Hz and [28–32] Hz bands.

Figures 3 and 4 show the change of channels contribution through the segment windows. For both classes, in Fig. 3 the highest channel contributions are at the MI period beginning. Nevertheless, the analysis finds highest channel contribution values in [24–36] Hz frequency band at the end of the trial. Regarding to Fig. 4, the highest contribution values appears at the frequency band [28–32] Hz.

In order to guarantee the interpretability in imagery motor tasks, the group analysis was carried out on brain synchronization information. Due to each subject has its own brain dynamics is necessary to include a group model that allows estimating similar patterns for all subjects. In this work, we used Group ICA and a connectivity analysis to perform this task. Group ICA is widely known and used to analyze tasks of multiple subjects through EEG. For both methods differents partens were found in the bands which are part of the rhythms μ and

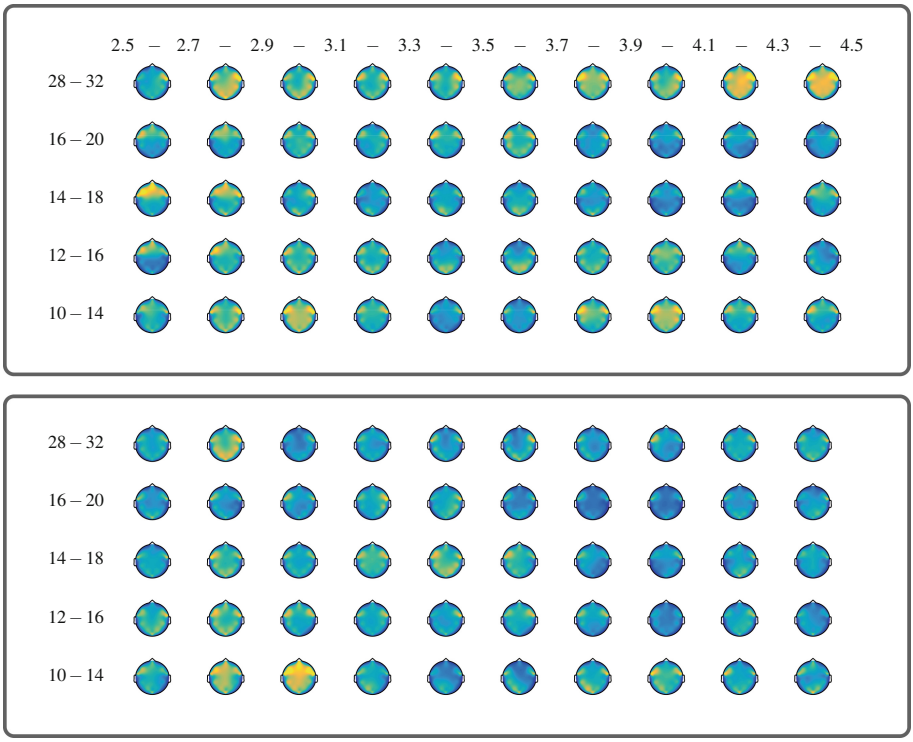

Fig. 4. Normalized time-frequency relevance values computed based on connectivity for all channels. Right class (first box) and left class (second box).

β frequencies which are known as sensorimotor rhythms. The obtained results on a concrete attention task show that the developed relevant connectivity analysis on group-level synchronization, improve the interpretation, although the proposed comparison for connectivity analysis depends on the time interval. As future work, we intend to validate EEG data with more complicated dynamics. To overcome more effectively nonstationarities of neural responses and structural homogeneity of latent processes across the sample, we plan to introduce an elaborate group-level strategy, including more complex approaches for graph analysis as well as enhanced relevance metrics.

Acknowledgements. This work is supported by the project Programa de reconstrucción del tejido social en zonas de pos-conflicto en Colombia del proyecto Fortalecimiento docente desde la alfabetización mediática Informacional y la CTel, como estrategia didáctico-pedagógica y soporte para la recuperación de la confianza del tejido social afectado por el conflicto. Código SIGP 58950 Financiado por Fondo Nacional de Financiamiento para la Ciencia, la Tecnología y la Innovación, Fondo Francisco José de Caldas con contrato No 213-2018 con Código 58960.

References

1. Hardmeier, M., Hatz, F., Bousleiman, H., Schindler, C., Stam, C.J., Fuhr, P.: Reproducibility of functional connectivity and graph measures based on the phase lag index (PLI) and weighted phase lag index (wPLI) derived from high resolution EEG. PloS One **9**(10), e108648 (2014)
2. Allison, B.Z., Wolpaw, E.W., Wolpaw, J.R.: Brain-computer interface systems: progress and prospects. Expert Rev. Med. Dev. **4**(4), 463–474 (2007)
3. Huster, R., Plis, S.M., Calhoun, V.D.: Group-level component analyses of EEG: validation and evaluation. Front. Neurosci. **9**, 254 (2015)
4. Allen, E., Damaraju, E., Eichele, T., Wu, L., Calhoun, V.D.: EEG signatures of dynamic functional network connectivity states. Brain Topogr. **31**(1), 101–116 (2018)
5. Labounek, R., et al.: Stable scalp EEG spatiospectral patterns across paradigms estimated by group ICA. Brain Topogr. **31**(1), 76–89 (2018)
6. Zhang, Y., Zhou, G., Jin, J., Wang, X., Cichocki, A.: Optimizing spatial patterns with sparse filter bands for motor-imagery based brain-computer interface. J. Neurosci. Methods **255**, 85–91 (2015)
7. Dai, S., Wei, Q.: Electrode channel selection based on backtracking search optimization in motor imagery brain-computer interfaces. J. Integr. Neurosci. **16**(3), 241–254 (2017)
8. Aviyente, S., Tootell, A., Bernat, E.M.: Time-frequency phase-synchrony approaches with ERPs. Int. J. Psychophysiol. **111**, 88–97 (2017)
9. Terrien, J., Germain, G., Marque, C., Karlsson, B.: Bivariate piecewise stationary segmentation; improved pre-treatment for synchronization measures used on non-stationary biological signals. Med. Eng. Phys. **35**(8), 1188–1196 (2013)
10. Reinhold Scherer, C.V.: Motor imagery based brain-computer interfaces, chap. 8, pp. 171 – 195 (2018)
11. Wolpaw, J.R., Birbaumer, N., McFarland, D.J., Pfurtscheller, G., Vaughan, T.M.: Brain-computer interfaces for communication and control. Clin. Neurophysiol. **113**(6), 767–791 (2002)